Journal of Catalysis 257 (2008) 382–389

Contents lists available at ScienceDirect

Journal of Catalysis

www.elsevier.com/locate/jcat

A kinetic study of benzene alkylation with ethane into ethylbenzene over bifunctional PtH-MFI catalyst

Dmitry B. Lukyanov [*], Tanya Vazhnova

Catalysis and Reaction Engineering Group, Department of Chemical Engineering, University of Bath, Bath, BA2 7AY, UK

ARTICLE INFO

Article history:
Received 17 November 2007
Revised 12 May 2008
Accepted 16 May 2008
Available online 16 June 2008

Keywords:
Ethane
Ethylbenzene
Dehydrogenation
Alkylation
Bifunctional catalysis
Zeolites

ABSTRACT

Benzene alkylation with ethane into ethylbenzene (EB) was studied at 370 °C over a PtH-MFI bifunctional catalyst of high acidity (Si/Al = 15). Highly selective and stable catalyst operation was observed at benzene conversions up to 10–12%, which are close to the thermodynamic equilibrium conversion value of 13.5%. Kinetic analysis of the experimental data reveals that EB is formed via two consecutive reaction steps: (i) ethane dehydrogenation into ethene over Pt sites and (ii) benzene alkylation with ethene over acid sites. These reactions dominate at low contact times and benzene conversions up to 10-12%. At higher conversions (i.e. higher contact times) other reactions start to compete with the EB formation steps leading to a steep drop in the EB selectivity and to a decrease in the catalyst stability. The analysis of these side reactions results in a better understanding of the requirements for the selective and stable benzene alkylation with ethane into EB over bifunctional zeolite catalysts.

© 2008 Elsevier Inc. All rights reserved.

1. Introduction

Ethylbenzene (EB) is a key intermediate in production of polystyrene and is annually produced in the amount of 23 million metric tons [1]. The current technologies of EB production [1,2] are based on the zeolite catalyzed benzene alkylation with ethene, which is produced in the steam reforming of ethane and naphtha [3]. Both latter processes are very energy intensive, consume fossil fuels and generate a greenhouse gas, CO_2 [3]. The replacement of ethene with ethane, as the alkylating agent in the synthesis of EB, would allow elimination of the ethene production step and, as a consequence, would lead to the commercial and environmental benefits in the EB production. Obviously, the new process, benzene alkylation with ethane into EB, would be commercially viable only if high EB selectivity and catalyst stability are achieved.

The possibility of the direct benzene alkylation with ethane into EB was first established by Olah et al. [4]. With fluoroantimonic acid (HF-SbF5) as a catalyst, the EB yield was 1 mol% and the selectivity to EB in the aromatic products was around 76 mol% [4]. Later on, several research groups investigated benzene alkylation with ethane [5–7] and propane [5,7–11] over a number of Pt- and Ga-containing zeolite catalysts, which are free from the corrosion and environmental problems associated with the superacidic catalytic systems. However, the zeolite-based catalysts produced mixtures of various alkyl and dialkylbenzenes with very low selectivities to the products of direct alkylation, i.e. EB and propylbenzenes (PB). The studies of benzene alkylation with ethane over bifunctional zeolite catalysts [5–7] were performed at 450–600 °C and showed the complexity of the reaction pathways at these temperatures. It was suggested [6,7] that EB was produced over acid sites via benzene alkylation with ethene, which was formed initially in ethane dehydrogenation over Pt sites. However, no attempt was made in these studies [5–7] to investigate experimentally the reaction pathways that led to the observed low EB selectivities.

In our recent paper [12] we have identified three groups of side reactions, namely, (i) ethane hydrogenolysis, (ii) reactions of alkenes and (iii) transformation of EB, which were likely responsible for the low EB selectivities previously reported for benzene alkylation with ethane over bifunctional zeolite catalysts. We then analyzed the thermodynamic and kinetic limitations associated with the target and side reactions. This analysis suggested that alkene reactions could be suppressed at lower temperatures and that EB formation steps and the steps of its transformation could be decoupled by using catalysts of low or moderate acidity [12]. This suggestion was then verified by the experiments on benzene alkylation with ethane at 370 °C over two PtH-MFI catalysts with the Si/Al ratios of 36 and 140. Both catalysts displayed a remarkably stable performance (during 45–49 h on stream) with EB selectivity in the aromatic products in the range between 92–95 mol% and the highest EB yield (benzene based) of 10.7 mol% [12].

Thus, our recent communication [12] has demonstrated for the first time the feasibility of the highly selective and stable alkylation of benzene with ethane into EB over bifunctional zeolite catalysts and suggested a number of reaction steps that may be involved

---

[*] Corresponding author. Fax: +44 1225 385713.
E-mail addresses: d.b.lukyanov@bath.ac.uk (D.B. Lukyanov), t.vazhnova@bath.ac.uk (T. Vazhnova).

0021-9517/$ – see front matter © 2008 Elsevier Inc. All rights reserved.
doi:10.1016/j.jcat.2008.05.020

in this complex reaction. The aim of the present study was to get further insight into the reaction pathways of benzene alkylation with ethane into EB over Pt-containing MFI catalysts. To achieve this goal, we conducted a detailed kinetic study of this reaction at 370 °C over a PtH-MFI zeolite catalyst with a Si/Al ratio of 15. This catalyst was chosen since it was of interest to verify if similar, highly selective and stable performance can be attained with a higher acidity catalyst when compared to the catalysts of lower acidity that were used previously [12].

2. Experimental

2.1. Catalyst preparation and characterization

A sample of H-MFI zeolite with a Si/Al ratio of 15 (ZEOLYST) was used in this work as a parent material. High crystallinity of the zeolite and the absence of other phases were confirmed by X-ray diffraction analysis. The size of the zeolite crystallites was in the range between 0.4 and 0.7 μm, as determined by scanning electron microscopy. The number of acid sites in the zeolite was determined by FTIR spectroscopy using pyridine as a probe molecule. FTIR spectra of the self-supported catalyst discs were collected at a resolution of 2 cm^{-1} using a Bruker Equinox 55 FTIR spectrometer and a purpose-built IR cell that allowed high-temperature treatment of samples in situ [13]. Pyridine adsorption was carried out at 150 °C, after activation of the samples under vacuum (10^{-5} mbar) at 400 °C overnight. These experiments revealed that the number of all acid sites in the H-MFI zeolite was 535 $\mu mol\,g^{-1}$, and that the numbers of the Brønsted and Lewis acid sites were 448 and 87 $\mu mol\,g^{-1}$, respectively.

The Pt-containing zeolite catalyst (1 wt% Pt), defined as PtH-MFI, was prepared by incipient wetness impregnation of the H-MFI zeolite with an aqueous solution of tetraammineplatinum(II) nitrate, $Pt(NH_3)_4(NO_3)_2$. After impregnation the catalyst was dried slowly at room temperature (∼48 h), and then calcined (in a thin layer) in a muffle furnace at 530 °C for 4 h (heating rate was 1 °C/min). For kinetic studies, the catalyst powder samples were pressed into disks, crashed, and sieved to obtain catalyst particle sizes in the range of 250–500 μm. The Pt dispersion in the PtH-MFI catalyst was 12%. It was determined on a purpose-built adsorption system (Johnson Matthey) from the uptake of strongly chemisorbed CO at 25 °C and assuming CO/Pt adsorption ratio of 1. Prior to CO adsorption experiments the catalyst samples (0.5 g) were first oxidized at 530 °C for 4 h in flowing air (30 ml/min), and then reduced at 500 °C for 1 h in a flow of pure H_2 (30 ml/min). Based on the assumption of the uniform Pt distribution (as spherical particles), the diameter of the Pt particles was calculated to be around 10 nm.

2.2. Kinetic studies

Alkylation of benzene with ethane was studied at atmospheric pressure in a continuous flow reactor at 370 °C with the feed comprised of ethane (90 mol%) and benzene (10 mol%). The reaction mixture was analyzed by on-line GC using Varian CP-3800 Gas Chromatograph, which was equipped with a molecular sieve 13X packed column and a thermal conductivity detector (TCD) for analysis of H_2, and a 25 m long PLOT Al_2O_3/KCl capillary column with a flame ionization detector (FID) for analysis of hydrocarbons (argon was used as a carrier gas in both columns). Identification of the retention times for different hydrocarbons was done using reference hydrocarbon mixtures. TCD was calibrated using gas mixtures with different H_2 concentrations. Prior to the kinetic experiments, the catalyst samples were heated (1 °C/min) in the reactor under flowing air (30 ml/min) to 530 °C and kept at this temperature for 4 h. Then the temperature was reduced to 200 °C and the catalyst sample was purged with N_2 (50 ml/min) for 1 h before switching to the flowing H_2 (60 ml/min). The catalyst sample was then heated (5°C/min) to 500 °C and kept at this temperature for 1 h before cooling the sample to the reaction temperature (370 °C).

Contact time (τ) was defined as $WHSV^{-1}$, where WHSV (h^{-1}) is the total weight hour space velocity of ethane and benzene. Different levels of conversions of benzene and ethane were obtained by performing experiments at different values of contact time that was changed in the range between 0.0018 and 0.65 h (variation of WHSV was in the range between 557 and 1.54 h^{-1}, respectively). To achieve such a variation in contact time, the experiments were performed with different catalyst loadings (18.5–1000 mg) and different mass flow rates of the reactants (1.54–10.3 g/h). Two quartz reactors with the inner diameters of 3 and 8 mm were used in the experiments with the low (18.5, 40 and 125 mg) and high (500 and 1000 mg) catalyst loadings, respectively. The absence of the mass transfer limitations, which could be due to the changes in the flow rates, were confirmed by the same results obtained at the same contact times using different catalyst loadings (40 and 125 mg) and flow rates (1.54 and 4.81 g/h). Time on stream (TOS) studies revealed stable catalyst performance during 30 h of the reaction at all contact times used in this work (see Section 3.3), and the analysis of the reaction pathways was performed on the basis of the experimental data obtained at TOS between 20 and 24 h.

3. Results and discussion

This section starts with consideration of the effect of contact time on ethane and benzene conversions and product selectivities, and then proceeds to the detailed analysis of the reaction pathways of benzene alkylation with ethane into EB over the PtH-MFI catalyst. This leads to the identification of the sequence of the main reaction steps, which are used later on in the discussion of the TOS experiments at the end of this section.

3.1. Effect of contact time on feed conversion and product selectivities

Fig. 1 shows that the conversions of benzene and ethane increase with growing contact time and reach their highest levels (21.5 and 5.8%, respectively) at the contact time of 0.65 h. It can be seen that the increase in benzene conversion is quite steep up to the level of about 10% ($\tau = 0.04$ h) and then slows down steadily at higher contact time values (Fig. 1). At the temperature of 370 °C, the reaction between benzene and ethane into ethylbenzene and hydrogen

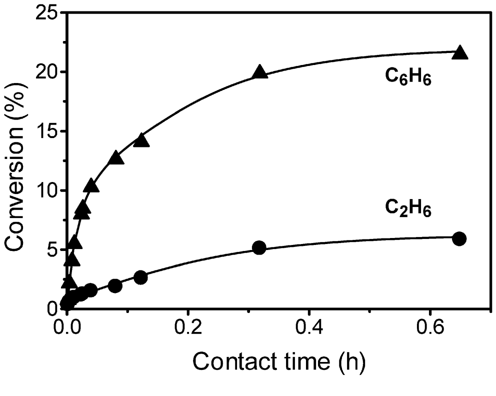

Fig. 1. Effect of contact time on benzene and ethane conversions over the PtH-MFI catalyst at 370 °C. Ethane to benzene molar ratio in the feed was 9:1, and the experimental data were obtained at TOS between 20 and 24 h.

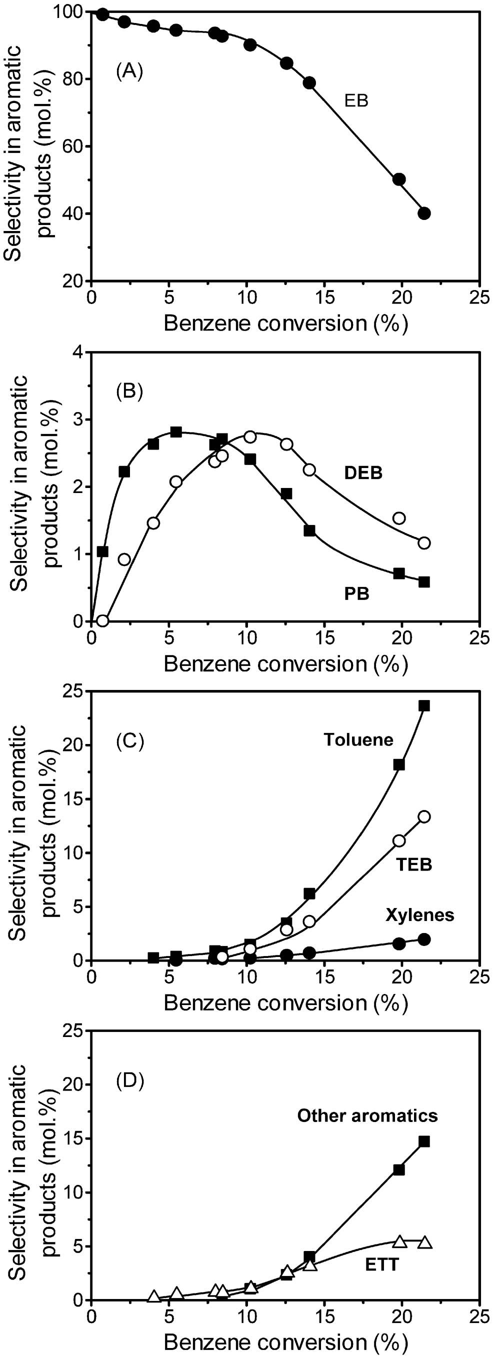

Fig. 2. Effect of benzene conversion on the selectivities in the aromatic products formed during benzene alkylation with ethane over the PtH-MFI catalyst at 370 °C: (A) EB; (B) DEB and PB; (C) toluene, xylenes and TEB; (D) ETT and other aromatics (C_{10}–C_{12} alkylbenzenes, naphthalene and its derivatives).

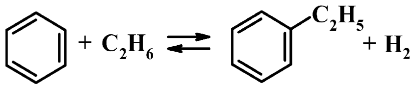

(1)

is strongly limited by thermodynamics, and the equilibrium conversion of benzene into EB is around 13.5%, as calculated on the basis of thermodynamic data [14] for the feed composition used in this work. Since the maximum benzene conversion (21.5%) observed in this work (Fig. 1) is essentially higher than the equilibrium benzene conversion into EB, one can conclude that benzene is transformed not only into EB but in other products as well.

This conclusion is fully supported by Fig. 2, which displays the selectivities to the aromatic products as functions of benzene conversion. Two distinct regions can be easily identified in Fig. 2. The first region corresponds to benzene conversions up to about 10% where EB selectivity in the aromatic products is very high (above 90 mol%) and decreases slowly with increasing conversion (Fig. 2A). From Fig. 2 it follows that this decrease is mainly associated with the rising selectivities to PB and diethylbenzenes (DEB). In the second region, at benzene conversions above 10%, a steep drop in EB selectivity is observed (Fig. 2A) indicating clearly that formation of other aromatic products from benzene is taking place. Figs. 2C and 2D reveal that these aromatic products include toluene, xylenes, triethylbenzenes (TEB), ethyltoluenes (ETT) and other aromatics, which include different alkylbenzenes, naphthalene and its derivatives. Based on these observations and taking into account the experimental data shown in Fig. 1, we can conclude that at low contact times (up to 0.04 h) the conversions of benzene and ethane are rising steeply mainly due to their transformation into EB and hydrogen, while at higher contact times the slow increase in the feed conversion is associated with formation of other products, which can be formed via reactions involving EB as discussed in Section 3.2.

3.2. Reaction pathways of benzene alkylation with ethane over PtH-MFI catalyst

To get better understanding of the reaction pathways of benzene alkylation with ethane, we decided to analyze formation of the reaction products at low and high contact times separately, since it appears that different reactions are taking place in these two regions.

3.2.1. Reaction steps at low contact times

In the region of low contact times the following products were observed: hydrogen, ethene, EB, diethylbenzenes, propene, propane, and propylbenzenes. The ratio of iso-propylbenzene (IPB) to *n*-propylbenzene (NPB) was in the range between 35 and 45. Fig. 3 shows the concentrations of these products as functions of contact time and demonstrates that hydrogen, ethene and EB are the major reaction products (note the difference in the scales between Figs. 3A and 3B). Analysis of the concentration curves in Fig. 3 allows us to conclude that hydrogen and ethene are the initial reaction products, while DEB, propene, propane and PB are the products of the secondary reaction steps. The situation is more complicated in the case of the EB formation steps, since Fig. 3A shows that EB is a secondary product formed via benzene alkylation with ethene (ethene concentration clearly passes through a maximum) but does not allow us to exclude the possibility of EB formation directly via benzene alkylation with ethane. This possibility was noted by Smirnov et al. [7] who proposed that ethane dehydrogenation and ethene protonation into carbenium ion may occur over Pt-acidic centers that allow the direct alkylation of benzene with ethane into EB (Eq. (1)).

In order to clarify the mechanism of EB formation, we considered the selectivities to hydrogen, ethene and EB as functions of ethane conversion. These selectivities are shown in Fig. 4 and demonstrate clearly that EB is the secondary reaction product and that it is not formed via direct alkylation of benzene with ethane over the PtH-MFI catalyst used in this work. Our selectivity data (Fig. 4) verify experimentally that EB formation proceeds via classical bifunctional mechanism [15] that involves two distinct active sites catalyzing two distinct reaction steps. First, ethane dehydrogenation into ethene and hydrogen (Eq. (2)) is taking place over Pt sites and this reaction is then followed by benzene alkylation with ethene into EB (Eq. (3)) over Brønsted acid sites (BAS) via formation of ethyl carbenium ions. It is worth noting that the above

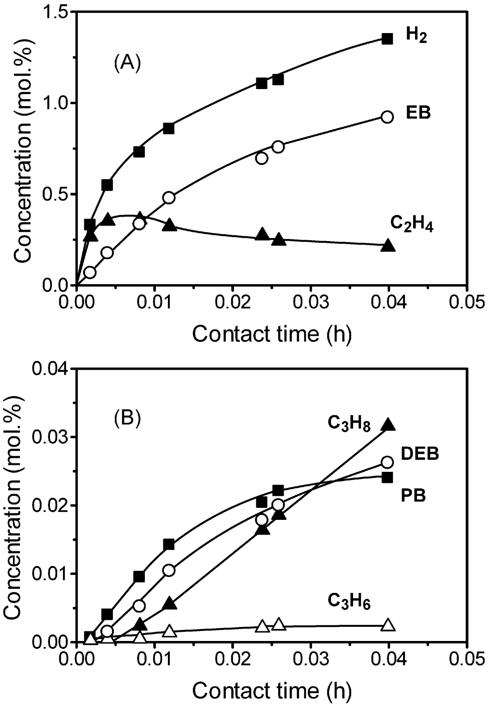

Fig. 3. Effect of contact time (in the region of low conversions) on the concentrations of (A) hydrogen, ethene and EB, and (B) propene, propane, PB and DEB formed during benzene alkylation with ethane over the PtH-MFI catalyst at 370 °C (ethane to benzene molar ratio in the feed was 9:1, and TOS was between 20 and 24 h). At contact time of 0.04 h, conversions of ethane and benzene were 1.51 and 10.3%, respectively.

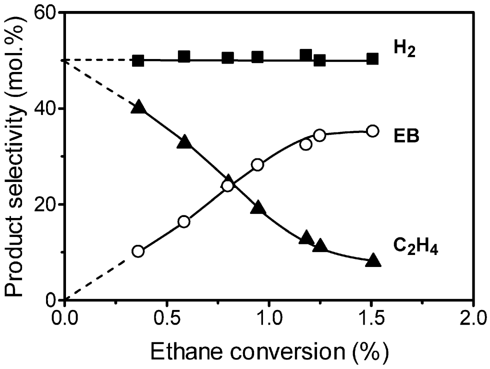

Fig. 4. Selectivities to hydrogen, ethene and EB as functions of ethane conversion over the PtH-MFI catalyst at 370 °C. Ethane conversion of 1.5% corresponds to benzene conversion of 10.3%. The sum of hydrogen, ethene and EB selectivities is 99.9 mol% at ethane conversion of 0.35% (isopropylbenzene and propene make together the remaining 0.1 mol%).

conclusion agrees well with the low Pt dispersion in our catalyst (12%). Indeed, it is clear that most of the Pt species are present in the catalyst as large particles (∼10 nm). Such Pt particles can be located only on the outer surface of the zeolite crystallites and, therefore, are spatially separated from BAS, which are located inside the channel system of the PtH-MFI catalyst.

$$C_2H_6 \rightleftarrows C_2H_4 + H_2 \qquad (2)$$

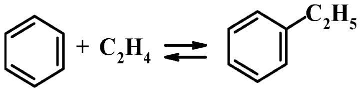 (3)

$$C_6H_6 + C_2H_4 \rightleftarrows C_6H_5C_2H_5 \qquad (3)$$

The kinetic study reported in this paper was carried out at 370 °C. At this temperature the equilibrium ethane dehydrogenation conversion into ethene (for pure ethane as feed) is around 0.55% [12]. Therefore, ethene concentration is very low at any point in the reactor and the whole process of EB formation is driven by benzene alkylation with ethene into EB (Eq. (3)) that withdraws ethene molecules from the reaction mixture and pushes ethane dehydrogenation (Eq. (2)) forward. The inherently low ethene concentration in the reactor hinders significantly the formation of all side reaction products (DEB, propene, propane and PB) that are observed at low contact times (see Fig. 3B). Indeed, it slows down the formation of diethylbenzenes that are formed via EB alkylation with ethene over BAS [1,2] as shown below.

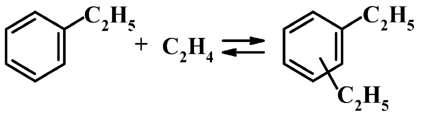 (4)

$$C_6H_5C_2H_5 + C_2H_4 \rightleftarrows C_6H_4(C_2H_5)_2 \qquad (4)$$

Also, the low ethene concentration leads to a significant decrease in the rates of the acid catalyzed bimolecular ethene dimerization steps (Eq. (5)). In our case, these steps are the initial steps in the sequence of alkene oligomerization and cracking reactions that produce different alkenes [16], as illustrated below by the reactions (6)–(8) for the formation of hexenes, pentenes and propene.

$$C_2H_4 + C_2H_4 \rightleftarrows C_4H_8 \qquad (5)$$

$$C_2H_4 + C_4H_8 \rightleftarrows C_6H_{12} \qquad (6)$$

$$C_6H_{12} \rightleftarrows C_3H_6 + C_3H_6 \qquad (7)$$

$$C_2H_4 + C_3H_6 \rightleftarrows C_5H_{10} \qquad (8)$$

According to the literature [17–19], alkene distribution resulting from the oligomerization and cracking reactions is a strong function of alkene partial pressure and is shifted to small alkenes at low alkene concentrations. Therefore, not only the rates of alkene reactions were suppressed under reaction conditions of this study, but the formation of the higher molecular weight alkenes was hindered as well. As a consequence, only ethene and propene were observed in the reaction mixture at low contact times. Formation of propene has led to formation of propane via platinum catalyzed hydrogenation reaction (9) and to formation of PB via acid catalyzed benzene alkylation reaction (10) as shown below.

$$C_3H_6 + H_2 \rightleftarrows C_3H_8 \qquad (9)$$

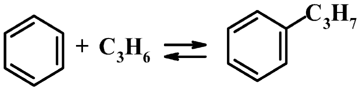 (10)

$$C_6H_6 + C_3H_6 \rightleftarrows C_6H_5C_3H_7 \qquad (10)$$

Quite obviously, the observed low concentrations of propane and propylbenzenes in the reaction mixture (Fig. 3B) can be explained by very low propene concentration that slowed down the rates of the reactions (9) and (10).

3.2.2. Reaction steps at high contact times

Fig. 5 shows the distribution of the products of benzene alkylation with ethane in the whole range of contact times used in this study. As contact time increases from 0.04 to 0.65 h, the new products are observed in the reaction mixture: methane (Fig. 5A); toluene and xylenes (Fig. 5C); ethyltoluenes, triethylbenzenes and other aromatics (Fig. 5D), which include different alkylbenzenes, naphthalene and its derivatives. Simultaneously with formation of these products a significant increase is observed for propane concentration (Fig. 5C), while the concentrations of EB, DEB and PB pass through the maximums (Figs. 5A and 5B). Analysis of the experimental data in Fig. 5 allows us to suggest a number of reaction steps that are responsible for the changes in the product concentrations at high contact times.

Formation of methane is clearly associated with formation of toluene via hydrogenolysis (hydrocracking) of EB over Pt sites of the catalyst

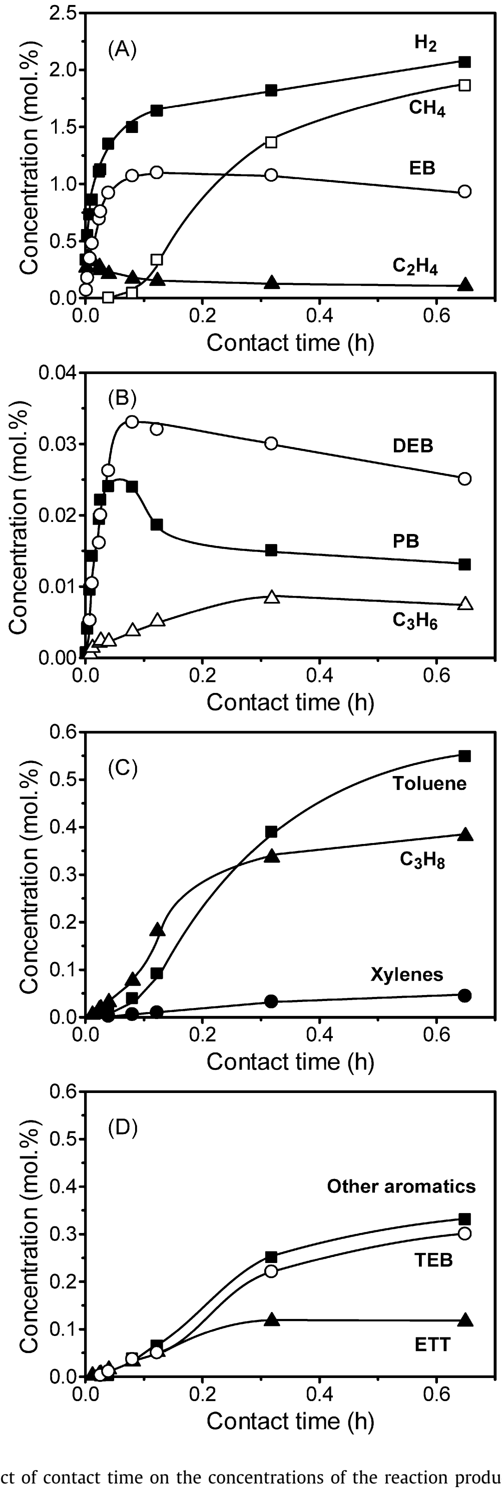

Fig. 5. Effect of contact time on the concentrations of the reaction products formed during benzene alkylation with ethane over the PtH-MFI catalyst at 370 °C: (A) hydrogen, methane, EB and ethene; (B) DEB, PB and propene; (C) toluene, xylenes and propane; (D) ETT, TEB and other aromatics (C_{10}–C_{12} alkylbenzenes, naphthalene and its derivatives). Ethane to benzene molar ratio in the feed was 9:1, and the experimental data were obtained at TOS between 20 and 24 h.

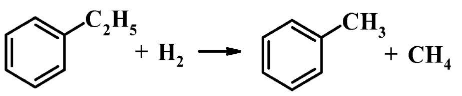
(11)

However, taking into consideration that methane is formed in essentially higher amounts than toluene (Figs. 5A and 5C), we can conclude that other hydrogenolysis reactions are taking place. The most likely reactions are shown below (reactions (12), (13), (14) and (15)). It is known (see, for example, the paper by Cortright et al. [20] and references therein) that hydrogenolysis reactions require several adjacent Pt sites. According to the data on the Pt dispersion (12%), our catalyst contains large Pt particles and, therefore, is likely to catalyze hydrogenolysis reactions (in particular, at high contact times that lead to higher ethane conversions and, as a consequence, to higher concentrations of H_2 in the reaction mixture).

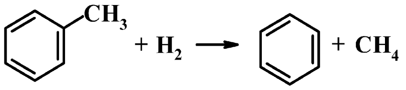
(12)

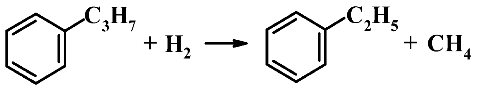
(13)

$$C_2H_6 + H_2 \rightarrow CH_4 + CH_4 \qquad (14)$$

$$C_3H_8 + H_2 \rightarrow C_2H_6 + CH_4 \qquad (15)$$

The experimental data of this work does not allow estimation of the relative contributions of the reactions (12)–(15) to methane formation, but it is worth noting that hydrogenolysis of toluene (reaction (12)) can by itself explain that methane is formed in higher amounts than toluene (Figs. 5A and 5C). Hydrogenolysis of PB (Eq. (13)) is likely to be responsible for the observed maximum in PB concentration (Fig. 5B), while EB hydrogenolysis (Eq. (11)) appears to be the main reaction that limits EB concentration (Fig. 5A). Another reaction, which can contribute essentially to EB transformation is the acid catalyzed EB alkylation with ethene into DEB (Eq. (4)). Indeed, Fig. 5D shows that this reaction is obviously followed by DEB alkylation with ethene into TEB as shown below.

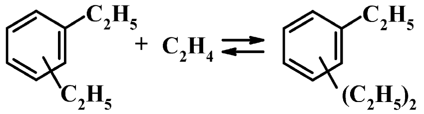
(16)

The latter reaction leads to the relatively high concentrations of TEB (Fig. 5D) and therefore requires essential amounts of EB, as a starting compound, for its production. It is very likely that TEB formation is responsible for the observed maximum in DEB concentration (Fig. 5B).

Formation of xylenes can be explained by EB hydroisomerization reaction

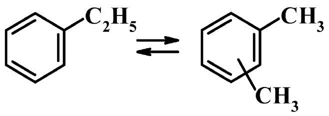
(17)

that proceeds via a sequence of reaction steps that occur over Pt and acid sites, as discussed by Moreau et al. [21] in their study of EB transformation over Pt containing mordenite catalysts.

Formation of ethyltoluenes is likely to occur via toluene alkylation with ethene over BAS (Eq. (18)) and DEB hydrogenolysis over Pt sites (Eq. (19)) as shown below.

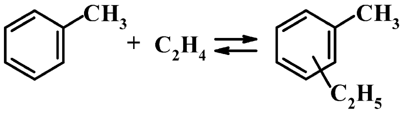
(18)

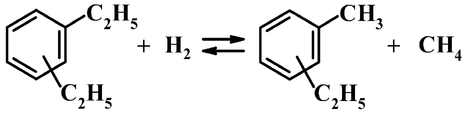
(19)

Alkylation of toluene with ethene (Eq. (18)) appears to be more important for ETT formation due to much higher toluene concentration in comparison with the concentration of DEB (Figs. 5B and 5C).

Finally, let us consider formation of other aromatic products (Fig. 5D) that include C_{10}–C_{12} alkyl and dialkylbenzenes, naphthalene and its derivatives. The term "C_{10}–C_{12} alkyl and dialkylbenzenes" is used in this paper to define aromatic molecules that contain 10–12 carbon atoms, i.e. benzene molecules substituted with relatively short alkyl groups. Most of the dialkylbenzenes were represented by ethylpropylbenzenes, which are clearly the products of the acid catalyzed EB alkylation with propene and PB alkylation with ethene

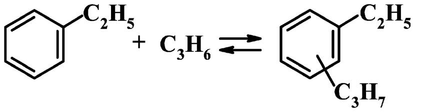

(20)

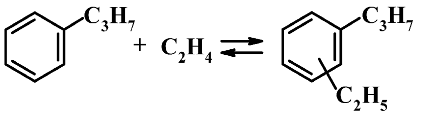

(21)

Formation of C_{10}–C_{12} alkylbenzenes at high contact time can be explained by benzene alkylation with butenes, pentenes and hexenes that are the products of alkene oligomerization and cracking reactions (Eqs. (5), (6) and (8)). Once formed, C_{10}–C_{12} alkylbenzenes can be transformed into naphthalene and its derivatives, which were also observed at high contact times. Based on the chemistry of the aromatization (dehydrocyclization) reactions established for the acid zeolite catalysts [19,22–24] and taking into consideration the presence of Pt sites in our MFI catalyst, we suggest that C_{10}–C_{12} alkylbenzenes undergo dehydrogenation over Pt sites (Eq. (22)) that is followed by cyclization and isomerization steps over BAS (Eq. (23)) and, finally, by the dehydrogenation steps catalyzed by Pt sites (Eq. (24)), as illustrated below for the transformation of pentylbenzene into methyl-naphthalene.

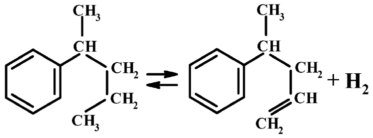

(22)

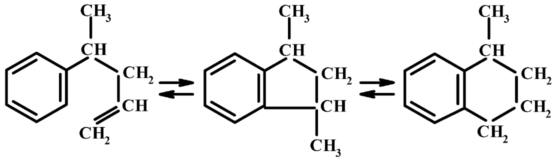

(23)

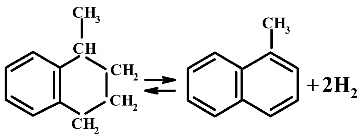

(24)

With purely acidic zeolite catalysts, formation of the hydrogen-deficient hydrocarbons, which are the products of the reactions (22) and (24), proceeds entirely via bimolecular hydrogen transfer (HT) steps with the involvement of carbenium ions formed by alkenes on BAS [19,22–24]. Thus, it is possible that the HT steps operate in parallel with the dehydrogenation steps in the case of bifunctional catalysts that contain both the metal and acid sites. The relative importance of these two routes in the dehydrocyclization reactions depends on the zeolite structure, number of metal and acid sites in the catalysts, and alkene concentration in the reaction mixture [16,25,26]. As discussed above, under the reaction conditions used in this work, the concentration of alkenes, which are required for the HT reactions, is very low at any point in the reactor. Therefore, it is likely that the dehydrogenation reactions (22) and (24) dominate in the formation of the hydrogen-deficient molecules (including naphthalene and its derivatives) that were observed in this study.

From Figs. 1 and 2D it follows that at contact time of 0.32 h (WHSV = 3.1 h^{-1}) C_{10}–C_{12} alkylbenzenes and naphthalenic compounds constituted about 12 mol% of all aromatic products formed over the PtH-MFI catalyst used in this work. Interestingly, under the same reaction conditions [12], formation of these aromatic compounds was not observed over the Pt-containing MFI catalysts with the Si/Al ratio of 36 and 140. It is likely that this difference is due to the lower acidity of the latter catalysts when compared to the PtH-MFI catalyst (Si/Al = 15) used in this work. Indeed, as shown above, C_{10}–C_{12} alkylbenzenes and naphthalenic compounds are formed via a long sequence of the reaction steps, some of which are catalyzed by the Pt sites (e.g. dehydrogenation steps) while the other proceed over BAS (e.g. alkylation steps, alkene oligomerization and cracking steps). As a consequence, formation of these aromatic compounds over the PtH-MFI catalysts of lower acidity is likely to occur at higher contact times, as compared to the highly acidic PtH-MFI catalyst used in this work.

3.3. Time on stream experiments

In order to investigate the stability of the PtH-MFI catalyst at different levels of the feed conversions, we performed three TOS experiments at different contact times. Fig. 6 shows the results of these experiments and reveals stable performance of the PtH-MFI catalyst during 45–46 h on stream at benzene conversions of ~8 and ~12%. For initial benzene conversion of 8%, no essential changes were observed in the product distribution and, as a consequence, the selectivity to EB in the aromatic products (see Fig. 7, the data corresponding to $\tau = 0.024$ h) was very stable during 45 h. For initial benzene conversion of 12% ($\tau = 0.081$ h), the EB selectivity was nearly constant during 28 h and then increased slightly (from ~ 84 to ~87%) during the following 18 h of the experiment (Fig. 7). Simultaneously with this increase a

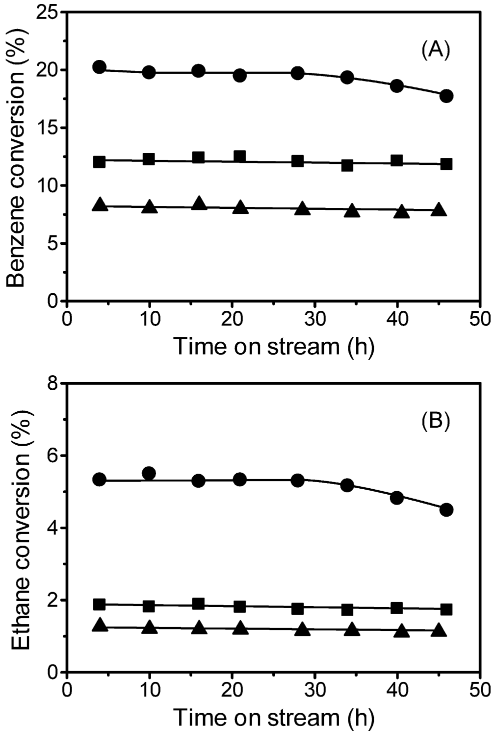

Fig. 6. Effect of time on stream on (A) benzene and (B) ethane conversions over PtH-MFI catalyst at contact times of (▲) 0.024, (■) 0.081 and (●) 0.32 h at 370 °C. Ethane to benzene molar ratio in the feed was 9:1.

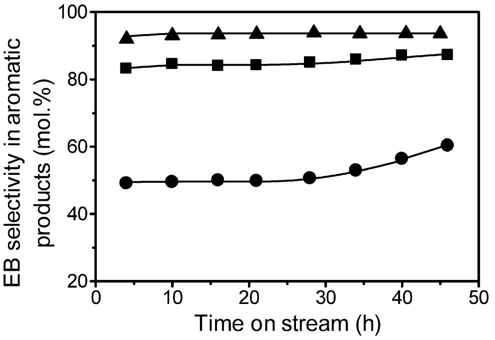

Fig. 7. Effect of time on stream on EB selectivity in aromatic products produced during benzene alkylation with ethane over PtH-MFI catalyst at contact times of (▲) 0.024, (■) 0.081 and (●) 0.32 h at 370 °C. Ethane to benzene molar ratio in the feed was 9:1.

Table 1
Comparison of the selectivities to aromatic products formed over the steady operating and partially deactivated PtH-MFI catalyst at benzene conversion of 17.5%

Catalyst	Steady operating[a]	Partially deactivated
Contact time (h)	0.21	0.32
Time on stream (h)	20–24	46
Benzene conversion (%)	17.5	17.4
Aromatics selectivity (mol%)		
Toluene	13.5	13.8
Ethylbenzene	60.5	60.3
Xylenes	1.3	1.1
Propylbenzenes	0.8	0.9
Ethyltoluenes	4.8	4.1
Diethylbenzenes	1.7	1.8
Triethylbenzenes	8.4	7.8
Other aromatics	9.0	10.2

[a] The data for the steady operating PtH-MFI catalyst at benzene conversion of 17.5% were obtained by interpolation of the experimental data shown in Figs. 1 and 2.

slight decrease was observed in the selectivities to toluene, ETT, TEB, C_{10}–C_{12} alkylbenzenes and naphthalenic compounds, which can be considered (according to Fig. 2) as the end aromatic products of the reaction over the PtH-MFI catalyst used in this study. These observations suggest that very slow coke formation is taking place in the PtH-MFI catalyst when benzene alkylation with ethane is carried out at the contact time of 0.081 h. The level of the catalyst deactivation is very low under these conditions, as evident from the fact that no noticeable changes have been observed in the conversions of benzene and ethane during 46 h of the reaction (Fig. 6).

At the initial benzene conversion of ~20% the PtH-MFI catalyst demonstrates stable performance during the first 28 h on stream (Figs. 6 and 7, the data corresponding to $\tau = 0.32$ h), but then a decrease in the conversions of benzene and ethane is observed. This decrease is possibly associated with a higher coking rate under these reaction conditions. In our view, that can be related to the enhanced formation (at high contact time) of C_{10}–C_{12} alkylbenzenes and naphthalenic compounds, which are usually considered as coke precursors in reactions over zeolite catalysts [23,27–30]. Indeed, the concentration of these compounds (Fig. 5D) correlates inversely with the stability of the catalyst performance in three TOS experiments that were carried out at different contact times (Figs. 6 and 7). This observation agrees well with our previous results on very stable operation of two PtH-MFI catalysts of lower acidity [12] when formation of C_{10}–C_{12} alkylbenzenes and naphthalenic compounds was not observed at all.

The deactivation of the PtH-MFI catalyst, which was used in this work, was observed at the contact time of 0.32 h between 28 and 46 h on stream. During this time ethane conversion decreased from 5.3 to 4.5%, while benzene conversion declined from 20 to 17.4% (Fig. 6). The decrease in the feed conversion was accompanied by an increase in the EB selectivity in the aromatic products (Fig. 7) that changed from ~50 to ~60 mol% between 28 and 46 h on stream. Thus, the deactivation of the catalyst active sites has led to the gain in the EB selectivity of ~10 mol%. Consideration of the data in Fig. 2A shows that practically the same change in the EB selectivity is observed when benzene conversion is changing between 17.5 and 20% due to the increase in contact time. In both cases (catalyst deactivation and variation of contact time), the increase in the EB selectivity is associated with decreasing selectivities to toluene, TEB, ETT, and C_{10}–C_{12} alkylbenzenes and naphthalenic compounds. Table 1 compares the aromatic product selectivities observed over the steady working and partially deactivated PtH-MFI catalyst at benzene conversion of 17.5%. The comparison reveals that catalyst deactivation and variation of contact time have very similar effects on the distribution of the aromatic products. This suggests that there is no preferential deactivation of the Pt or acid sites in the PtH-MFI catalyst used in this work, and that the deactivation simply leads to a decrease in "effective" contact time due to the decrease in the number of active sites available for the reaction. Further studies are in progress to verify this suggestion and get better understanding of the coke formation and its effect on the Pt and acid sites present in the PtH-MFI catalyst.

4. Conclusions

This study demonstrates for the first time that highly selective and stable benzene alkylation with ethane into EB can be achieved (Figs. 2, 6 and 7) with the highly acidic PtH-MFI catalyst at 370 °C at benzene conversions up to 10–12%, which are close to the equilibrium benzene conversion of 13.5%. Analysis of the product selectivities (Fig. 4) confirms the suggestion made earlier [6,7,12] that EB is formed via the sequence of two reaction steps: (i) dehydrogenation of ethane into ethene over Pt sites and (ii) benzene alkylation with ethene over acid sites. These two reactions control transformation of both the ethane and benzene at low contact times up to benzene conversions of ~10% due to the low rates of many side reactions. Some of these reactions (such as ethane and EB hydrogenolysis) are slow because of the relatively low hydrogenolysis activity of the PtH-MFI catalyst used in this work, while the other (such as reactions of alkenes) are suppressed by the inherently low ethene concentration at 370 °C. With further increase in benzene conversion (due to the increase in contact time) the selectivity of benzene transformation into EB drops steeply and is about 40 mol% at benzene conversion of 21.5% (Fig. 2A). It is shown that this loss of the EB selectivity is associated with a number of side reactions that take place at high contact times. The main side reactions include EB hydrogenolysis into toluene and methane, EB alkylation with ethene into DEB and TEB, formation of C_{10}–C_{12} alkylbenzenes and naphthalenic compounds. The latter compounds are likely to be responsible for slow deactivation of the PtH-MFI catalyst that was observed in this work at benzene conversion of ~20% after 28–30 h on stream.

Analysis of the reaction pathways allows us to conclude that four requirements should be met in order to achieve highly selective and stable benzene alkylation with ethane into EB over bifunctional zeolite catalysts. These requirements include: (i) the low hydrogenolysis activity of the catalyst; (ii) the low concentration of alkenes in the reactor; (iii) the decoupling of the steps of EB formation and the steps of its further transformation; and (iv) the elimination (prevention) of the steps of formation of C_{10}–C_{12} alkylbenzenes and naphthalenic compounds.

Acknowledgments

We thank Dr. Paul Millington (Johnson Matthey) for analysis of the Pt dispersion and valuable comments, and Dr. Sean Rigby (University of Bath) and Dr. Stan Golunski (Johnson Matthey) for helpful discussions. This work was supported by the Engineering and Physical Sciences Research Council of the UK (grant EP/C532554).

References

[1] T.F. Degnan Jr., C.M. Smith, C.R. Venkat, Appl. Catal. A: Gen. 221 (2001) 283.
[2] C. Perego, P. Ingallina, Catal. Today 73 (2002) 3.
[3] J.A. Moulijn, M. Makkee, A. van Diepen, Chemical Process Technology, John Wiley & Sons, Chichester, 2001, chapter 4.
[4] G.A. Olah, P. Schiiling, J.S. Staral, Yu. Halpern, J.A. Olah, J. Am. Chem. Soc. 97 (1975) 6807.
[5] S.A. Isaev, T.V. Vasina, O.V. Bragin, Izv. Akad. Nauk USSR, Ser. Khim. 10 (1991) 2228 (in Russian).
[6] S. Kato, K. Nakagawa, N. Ikenaga, T. Suzuki, Catal. Lett. 73 (2001) 175.
[7] A.V. Smirnov, E.V. Mazin, O.A. Ponomoreva, E.E. Knyazeva, S.N. Nesterenko, I.I. Ivanova, in: A. Galarneau, F. Di Renzo, F. Fajula, J. Vedrine (Eds.), Proc. 13th Intern. Zeolite Conf., CD-ROM edition, 25-O-05;
A.V. Smirnov, E.V. Mazin, O.A. Ponomoreva, E.E. Knyazeva, S.N. Nesterenko, I.I. Ivanova, Stud. Surf. Sci. Catal. 135 (2001) 153.
[8] I.I. Ivanova, N. Blom, E.G. Derouane, J. Mol. Catal. A: Chem. 109 (1996) 157.
[9] E.G. Derouane, H. He, S.B. Derouane-Abd Hamid, D. Lambert, I. Ivanova, J. Mol. Catal. A: Chem. 158 (2000) 5.
[10] A.V. Smirnov, E.V. Mazin, V.V. Yuschenko, E.E. Knyazeva, S.N. Nesterenko, I.I. Ivanova, L. Galperin, R. Jensen, S. Bradley, J. Catal. 194 (2000) 266.
[11] C. Bigey, B.-L. Su, J. Mol. Catal. A: Chem. 209 (2004) 179.
[12] D.B. Lukyanov, T. Vazhnova, J. Mol. Catal. A: Chem. 279 (2008) 128.
[13] V.L. Zholobenko, M.A. Makarova, J. Dwyer, J. Phys. Chem. 97 (1993) 5962.
[14] D.R. Stull, E.F. Westrum Jr., G.C. Sinke, The Chemical Thermodynamics of Organic Compounds, John Wiley & Sons, New York, 1969.
[15] P.B. Weisz, in: D.D. Eley, P.W. Selwood, P.B. Weisz (Eds.), Advances in Catalysis and Related Subjects, Academic Press, New York, 1962, p. 137.
[16] D.B. Lukyanov, N.S. Gnep, M.R. Guisnet, Ind. Eng. Chem. Res. 33 (1994) 223.
[17] W.E. Garwood, in: G.D. Stucky, F.G. Dwyer (Eds.), ACS Symposium Series, vol. 218, American Chemical Society, Washington, DC, 1983, p. 383.
[18] W.O. Haag, in: D.H. Olson, A. Bisio (Eds.), Proc. Sixth Intern. Zeolite Conf., Butterworths, Surrey, UK, 1984, p. 466.
[19] R.J. Quann, L.A. Green, S.A. Tabak, F.J. Krambeck, Ind. Eng. Chem. Res. 27 (1988) 565.
[20] R.D. Cortright, R.M. Watwe, B.E. Spiewak, J.A. Dumesic, Catal. Today 53 (1999) 395.
[21] F. Moreau, N.S. Gnep, S. Lacombe, E. Merlen, M. Guisnet, Appl. Catal. A: Gen. 230 (2002) 253.
[22] M.L. Poutsma, in: J.A. Rabo (Ed.), Zeolite Chemistry and Catalysis, in: ACS Monograph, vol. 171, ACS, Washington, DC, 1976, p. 437.
[23] J.C. Vedrine, P. Dejaifve, E.D. Garbowski, E.G. Derouane, Stud. Surf. Sci. Catal. 5 (1980) 29.
[24] H. Pines, Chemistry of Catalytic Hydrocarbon Conversions, Academic Press, New York, 1981, chapter 1.
[25] D.B. Lukyanov, N.S. Gnep, M.R. Guisnet, Ind. Eng. Chem. Res. 34 (1995) 516.
[26] D.B. Lukyanov, T. Vazhnova, Appl. Catal. A: Gen. 316 (2007) 61.
[27] L.D. Rollmann, D.E. Walsh, J. Catal. 56 (1979) 139.
[28] D.E. Walsh, L.D. Rollmann, J. Catal. 56 (1979) 195.
[29] E.G. Derouane, Stud. Surf. Sci. Catal. 5 (1980) 5.
[30] M. Guisnet, P. Magnoux, Appl. Catal. A: Gen. 212 (2001) 83.